

# STRUCTURE AND MECHANICAL PROPERTIES OF 2219-T87 ALUMINIUM ALLOY JOINTS PRODUCED BY FLASH BUTT WELDING

**S.I. Kuchuk-Yatsenko, K.V. Hushchyn, I.V. Ziakhor,  
S.M. Samotryasov, M.S. Zavertannyi and A.M. Levchuk**  
E.O. Paton Electric Welding Institute of the NAS of Ukraine

11 Kazymyr Malevych Str., 03150, Kyiv, Ukraine. E-mail: [office@paton.kiev.ua](mailto:office@paton.kiev.ua)

During designing and manufacture of aircraft structures from modern thermomechanically strengthened aluminium alloys, there is a problem of producing welded joints with satisfactory mechanical properties without post heat treatment of large-sized products. In the work the formation of joints of thermomechanically strengthened 2219-T87 alloy during flash butt welding was investigated. It was found that a low-temperature resistance heating in combination with a short-term heating by flashing provide the formation of defect-free welded joints. Metallographic examinations showed that joints are formed through a thin layer of melt, which is a necessary condition for a high-quality welding of aluminium alloys. The influence of intense plastic deformation during upsetting with a forced formation on the morphology of  $\theta$ -phase ( $\text{CuAl}_2$ ) particles was studied. A decrease in the values of hardness in the joint area as a result of dissolution and coagulation of a strengthening  $\theta'$ -phase was established. The strength of welded joints both along and across the rolled metal lines amounts to 76 % of the strength of the base metal. 20 Ref., 2 Tables, 7 Figures.

*Keywords:* 2219 aluminium alloy, flash butt welding, welded joint, mechanical properties

In the design of space and aircraft engineering, thermally strengthened aluminium alloys of the Al–Cu system are widely used [1]. 2219 alloy and its analogue 1201 alloy have been successfully used for structural elements operating at low temperatures, in particular for the manufacture of fuel tanks and load-carrying structural elements of the rockets Saturn V, Apollo, Space Shuttle, Ariane V and «Buran» [2].

To achieve the maximum level of strength, the workpieces of 2219 alloy are delivered in a thermomechanically strengthened state T87, which is achieved by heat treatment on a solid solution by deformation strengthening and a subsequent artificial ageing [3–6].

In the manufacture of products for aircraft and space engineering from 2219 alloy, different methods of welding (electron beam [7], argon arc with consumable [8–10] and nonconsumable electrode [11, 12], friction stir (FSW) [12–18] and flash butt welding [19, 20]) are used, which differ in the thermal cycle and the level of reduction of the mechanical properties of the metal in the heat-affected zone (HAZ). For example, the joints of 2219-T87 alloy, made by argon arc welding with consumable and nonconsumable electrode and FSW, have a tensile strength of 0.6–0.65 from the level of the base metal values [8–18], which is predetermined by a full dissolution

of particles of nanosized strengthening  $\theta'$ -phase in the weld and the HAZ.

In addition, the thermal cycle of welding products of 2219 alloy can reduce the corrosion resistance of the joints as a result of coagulation (coarsening) of  $\theta$ -phase particles ( $\text{SiAl}_2$ ) in the near-weld zone. The problem of reducing indices of mechanical properties and characteristics of corrosion resistance of welds as a result of liquation in the fusion zone while using the methods of fusion welding was studied in [7–12] and while using FSW in [13–18].

In particular, in [8–12] it was found that during argon arc welding of 2219 alloy with a nonconsumable electrode, in the near-weld zone, a eutectic reaction between the particles of  $\theta$ -phase ( $\text{CuAl}_2$ ) and  $\alpha$ -matrix of the alloy:  $\alpha + \theta \rightarrow L_E$  with the formation of liquid phase  $L_E$  at the eutectic temperature  $T_E = 548$  °C and higher occurs. Liquation around the large  $\theta$ -particles leads to an increase in their size and the formation of the  $\alpha$ -matrix of the alloy areas with a lower copper concentration. Liquation of copper at grain boundaries leads to the appearance of a split eutectic, which consists of bands with a high concentration of Cu (up to 33 at.%) and adjacent areas of the  $\alpha$ -phase with a low content of Cu, which causes a decrease in the corrosion resistance and mechanical properties of welds

S.I. Kuchuk-Yatsenko — <https://orcid.org/0000-0002-1166-0253>, K.V. Hushchyn — <https://orcid.org/0000-0003-3298-4537>,  
I.V. Ziakhor — <https://orcid.org/0000-0001-7780-0688>, S.M. Samotryasov — <https://orcid.org/0000-0003-4891-9625>,  
M.S. Zavertannyi — <https://orcid.org/0000-0002-8415-8555>, A.M. Levchuk — <https://orcid.org/0000-0002-0361-7394>

© S.I. Kuchuk-Yatsenko, K.V. Hushchyn, I.V. Ziakhor, S.M. Samotryasov, M.S. Zavertannyi and A.M. Levchuk, 2021

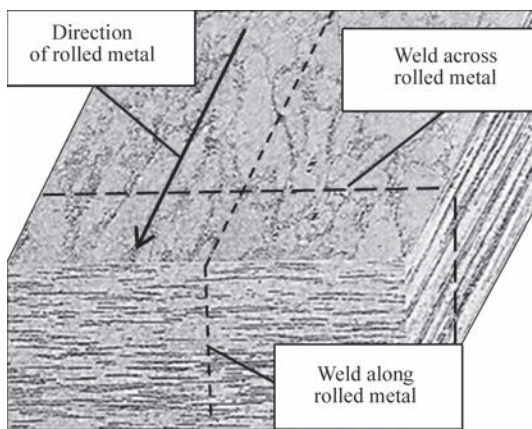


**Figure 1.** Scheme of rolled metal lines in the specimens of 2219-T87 alloy during FBW

[8–10]. The similar problems occur also during FSW of 2219 alloy [13–15].

Heat treatment (hardening and ageing) of products from 2219 alloy after welding allows a significant restoration of the structure and mechanical properties of the welds, but in the production of large-sized structures, such a task can hardly be realized. Therefore, the urgent problem is the development of technologies for welding of 2219 alloy, which provide a higher level of strength of joints without a post heat treatment, which will meet the technical requirements of space engineering developers.

An effective technology for the manufacture of load-carrying aircraft elements (stringers, shells, frame rings) from extruded profiles of developed and compact cross-section is flash butt welding (FBW). This method provides a high stable quality of joints, unites assembly and welding operations in a single cycle, does not demand application of consumables [19, 20]. In welding of billets of up to 12 mm thickness, the FBW technology provides high indices of strength of aluminium alloys at an insignificant width of the HAZ.

In FBW of profiles of a larger thickness it is necessary to carry out resistance preheating of billets, which causes an increase in width of HAZ and, probably, emergence of the problems characteristic of methods of fusion welding and FSW.

The aim of the work consisted in establishing the features of the formation of joints at FBW of thick-walled extruded profiles of 2219-T87 alloy, the study of their microstructure and determination of mechanical properties.

**Procedure of works.** The investigations were carried out on the specimens of 2219-T87 alloy of a

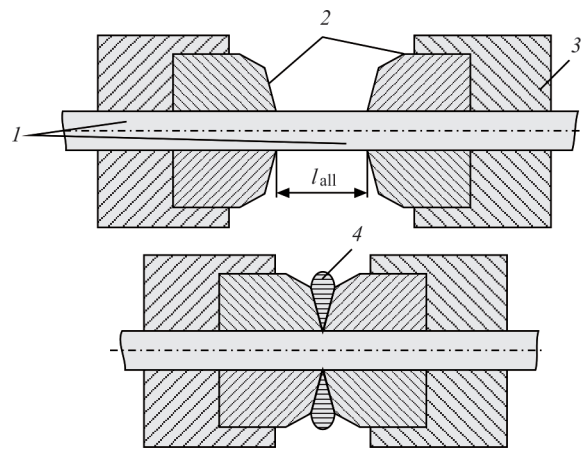


**Figure 2.** Scheme of FBW with the joint formation: 1 — parts; 2 — forming devices; 3 — current conductor; 4 — extruded metal;  $l_{all}$  — allowance for welding

rectangular section with 15 mm thickness and 60 mm width. The length of the specimens was not less than 200 mm. The chemical composition of the studied alloy is given in Table 1.

Since anisotropy of the structure and mechanical properties is characteristic for pressed profiles from aluminium alloys, the experiments on FBW of the specimens of 2219-T87 alloy were carried out at different direction of the rolled metal lines (Figure 1), which represent the clusters of  $\theta$ -phase particles. During welding of billets with a longitudinal arrangement of rolled metal fibers, the joint is formed in a plane perpendicular to the direction of rolled metal fibers (further, weld across the rolled metal). During welding of billets with a transverse arrangement of rolled metal fibers, the joints are formed in a plane parallel to the direction of rolled metal fibers (further, weld along the rolled metal).

Experimental welding was carried out in a laboratory flash butt welding machine K607, equipped with a welding transformer with a capacity of 75 kV·A and an upsetting drive with a force of up to 1000 kN. The FBW process included several stages: resistance preheating, flashing and upsetting. Deformation during upsetting occurs in the conditions of volume compression with the help of forming devices (Figure 2).

The parameters of the FBW process were established within the ranges: flashing voltage  $U_{2fl} = 5-6$  V, flashing rate  $V_{fl} = 2-18$  mm/s, upsetting rate  $V_{ups} \geq 200$  mm/s. The total allowance for flashing and upsetting is  $l_{all} = 60$  mm.

Macrostructure of welded joints was evaluated by visual inspection using the magnification glass Levenhuk Zeno Multi ML7 at a magnification

**Table 1.** Chemical composition (wt.%) of 2219 alloy [4, 5]

Al	Cu	Mn	Mg	Si	Zr	V	Zn	Fe	Ti
Base	5.8–6.8	0.2–0.4	<0.2	<0.2	0.1–0.25	0.05–0.15	<0.1	<0.3	0.02–0.1

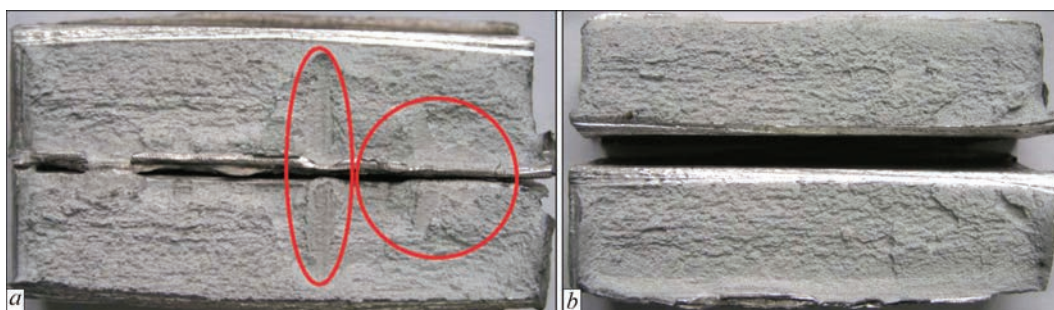


**Figure 3.** Fractures of welded joints: *a* — with defects (oxide films); *b* — without visible defects

of  $\times 3$ – $10$ . Metallographic examinations were performed with the use of an optical microscope Neophot-32 at a magnification of  $\times 25$ ,  $\times 100$  and  $\times 400$ . The preparation of the surface of macrosections was carried out in a grinding-polishing machine Struers LaboPol-5. To reveal the structure, Keller reagent ( $0.5\text{HF}-1.8\text{HC1}-2.7\text{HNO}_3-95\text{H}_2\text{O}$  (vol.%) and a 5 % aqueous solution of hydrofluoric acid were used. The study of the distribution of hardness *HRB* in the joint zone was carried out using a stationary hardness meter Novotest TS-BPR at a load of 600 N (ball diameter is  $1/16''$ ) with a step of 1–2 mm. Mechanical tensile tests of specimens of welded joints were carried out in the TsDM-10 machine with a maximum force of 100 kN.

**Results of investigations.** During welding, preheating resistance to  $200\text{ }^\circ\text{C}$  was used, the current of is  $I_{2\text{pr}} = 20\text{ kA}$ . Heating to this temperature does not lead to a

loss of the strength of 2219-T87 alloy. Further increase in the temperature of a preheating results in an increase in the width of the zone in which the complete dissolution and coagulation of the nanosized strengthening  $\theta'$ -phase in the FBW process is observed, that causes a decrease in the strength of the alloy.

In the process of testing the welding modes, an «express analysis» of the quality of welded joints — bending of specimens with a notch along the joint line until fracture was performed. The quality of the joints was evaluated by the presence (absence) of defects such as oxide films during visual inspection of fractures of the destroyed specimen (Figure 3, *a*). When testing the FBW modes, we tried to minimize the time of welding in order to reduce the width of the HAZ joints of 2219-T87 alloy.

According to such procedure, the FBW modes were determined, that provide the absence of defects (Fig-

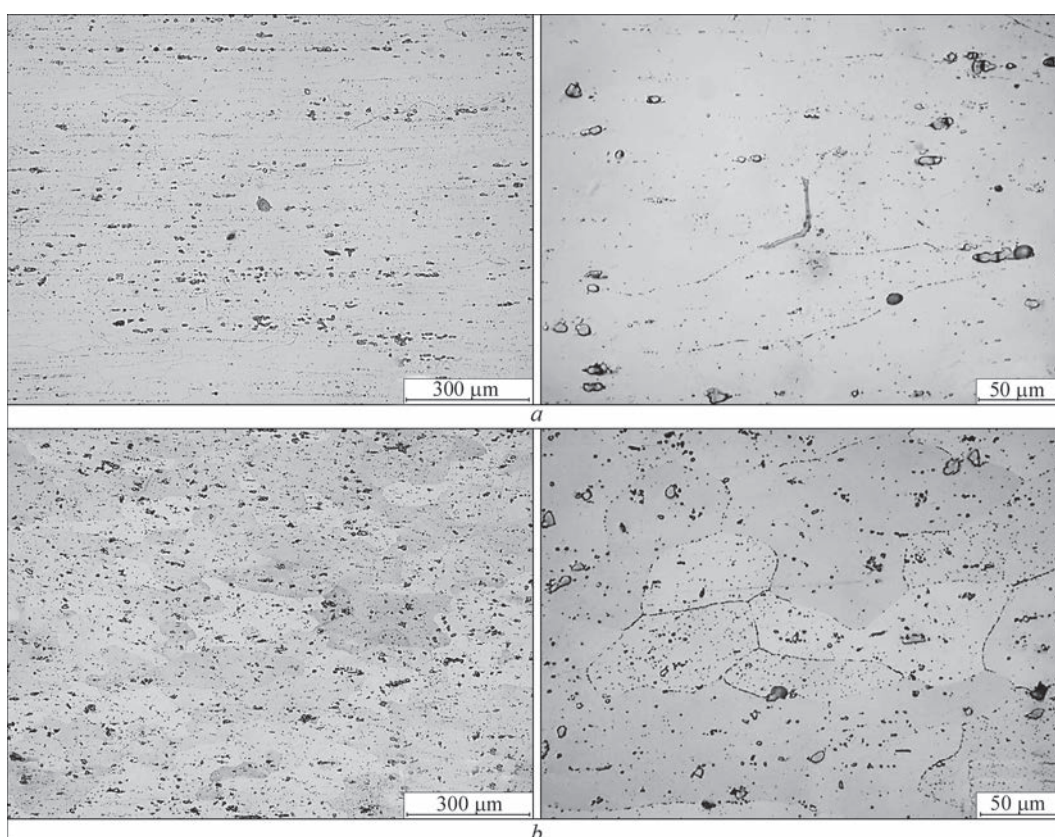


**Figure 4.** Microstructure of base metal of 2219-T87 alloy along (*a*) and across (*b*) the rolled metal

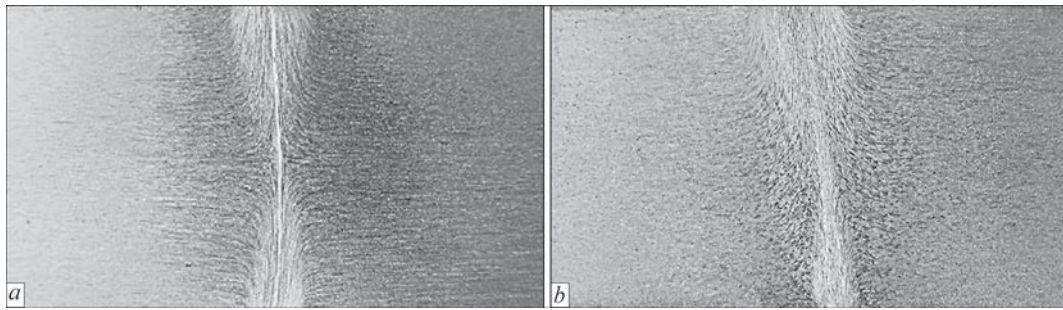


**Figure 5.** Structure of welded joint of specimens of 2219-T87 alloy: thickness  $\delta = 15$  mm: *a* — weld across the rolled metal; *b* — weld along the rolled metal

ure 3, *b*) along the joint line. It was established that a low-temperature resistance heating to 200 °C with a subsequent flashing during 15 s and deformation at the value of upsetting pressure not lower than 500 MPa provide the formation of high-quality joints. After obtaining positive results, batches of specimens were welded for metallographic examinations and mechanical tests.

The results of examinations of the microstructure of the base metal (BM) and welded joints (WJ) made by FBW are shown in Figures 4–6. The base metal of 2219-T87 alloy (Figure 4) is characterized by a pronounced texture with the grains deformed in the direction of the rolled metal and a large number of  $\theta'$ -phase particles ( $\text{CuAl}_2$ ) of different sizes, arranged in

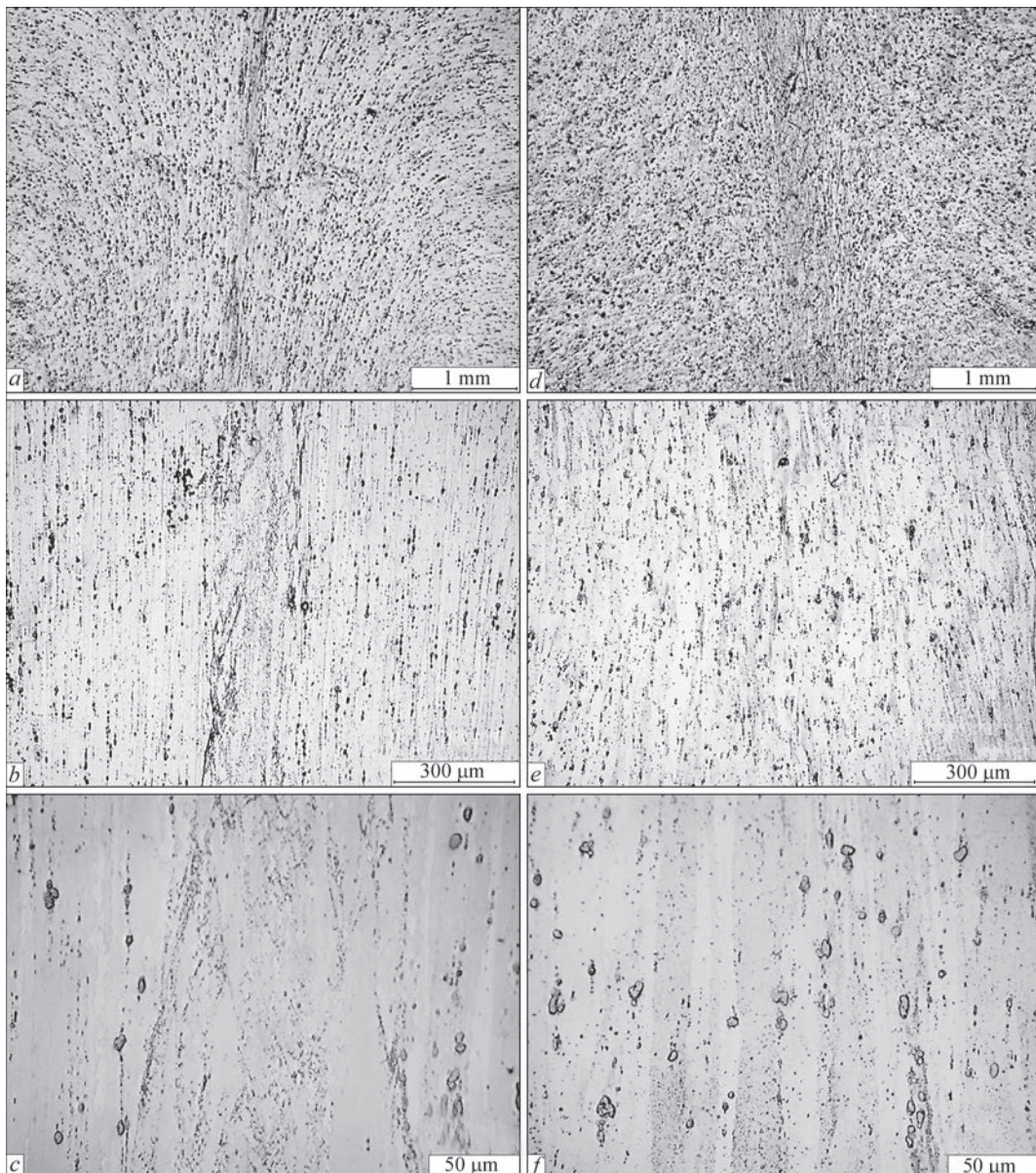


**Figure 6.** Microstructure of welded joint of 2219-T87 alloy of weld across (*a–c*) and along the rolled metal (*d–f*)

**Table 2.** Mechanical properties of base metal and welded joints of 2219-T87 alloy depending on the direction of the rolled metal

Specimen	$\sigma_t$ , MPa	$\sigma_{0.2}$ , MPa	$\delta_5$ , %	Bending angle $\alpha^\circ$	KCV, J/cm <sup>2</sup> ( $T = 20^\circ\text{C}$ )	Strength coefficient $\sigma_{t\text{WJ}}/\sigma_{t\text{BM}}$
Weld across the rolled metal						
BM	486	413	10.9	37	13.9	—
WJ	372	263	4.3	33	16.6	0.76
Weld along the rolled metal						
BM	486	410	8.0	21	6.9	—
WJ	372	249	5.0	31	20.5	0.76

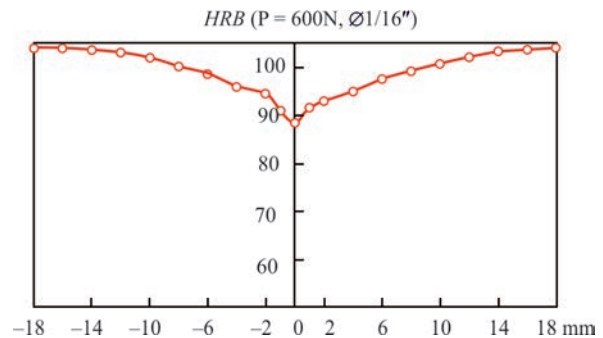
the form of «chains», the largest particles have a size of 10–15  $\mu\text{m}$ .

Approaching the joint line, a change in the orientation of the grains is observed, and the direction of rolled metal fibers in the zone of thermomechanical effect (ZTME) gradually changes to  $90^\circ$  as compared to the initial direction of BM grains and coincides with the direction of metal extrusion during upsetting deformation (Figure 6). As a result of metal extrusion into the gap between the forming devices, the  $\theta$ -phase precipitations are partially dissolved in ZTME — their size decreases, clusters in the form of «chains» are partially destroyed, the particles become separated. Such structure indicates a significant effect of intense plastic deformation during upsetting with a forced formation (extrusion) on the morphology of secondary phase precipitates.

In the welded joint both across (Figure 6, *a-c*) as well as along the rolled metal (Figure 6, *d-f*), such defects as oxide films, delaminations and eutectic formations are absent. In HAZ coarsening of  $\theta$ -phase particles ( $\text{CuAl}_2$ ) and the emergence of a split eutectic are not observed, which is characteristic for the methods of fusion welding [7–12] and FSW [13–18] of 2219 alloy.

The size of the  $\theta$ -phase particles in the center of the butt (joint area with a width of 150–200  $\mu\text{m}$ ) is 1–2  $\mu\text{m}$ , which is much smaller than that for BM of the alloy, and indicates the complete dissolution of the particles during welding and their repeated precipitation in a more dispersed form during cooling. Analysis of the microstructure (Figure 6) shows the formation of the joint through a thin layer of melt, which is a necessary condition for a high-quality welding of aluminium alloys.

Analysis of the hardness distribution in the joint zone of 2219-T87 alloy (Figure 7) shows that the width of the HAZ is about 28 mm. The decrease in hardness values is predetermined by structural transformations in the joint zone of 2219-T87 alloy under the influence of the FBW thermal cycle, namely by the dissolution and coagulation of nanosized strengthening of the  $\theta'$ -phase.

**Figure 7.** Hardness distribution in the welded joint zone of 15 mm thick specimens from 2219-T87 alloy

The results of tensile tests of BM of 2219-T87 alloy and welded joints are given in Table 2. Therefore, the tensile strength  $\sigma_t$  of the welded joints of the plates with a thickness of 15 mm from 2219-T87 alloy, produced by FBW, is 76 % of the strength values of the BM alloy both with the arrangement of the weld along and across the rolled metal.

## Conclusions

1. It was established that a resistance preheating of specimens of 2219-T87 alloy to a temperature of  $200^\circ\text{C}$  and conducting FBW with a forced formation under pressure value at an upsetting of not lower than 500 MPa, provide the formation of high-quality (defect-free) joints.

2. The microstructure of the metal in ZTME of the joint of 2219-T87 alloy indicates a significant effect of intense plastic deformation during upsetting with a forced formation on the morphology of  $\theta$ -phase particles ( $\text{CuAl}_2$ ). As a result of extrusion of the metal in a gap between the forming devices, a partial dissolution of the  $\theta$ -phase particles occurs — their size decreases, clusters in the form of «chains» are partially destroyed.

3. The size of the  $\theta$ -phase particles in the center of the joint zone with a width of 150–200  $\mu\text{m}$  is 1–2  $\mu\text{m}$ , which is predetermined by the complete dissolution of the  $\theta$ -phase during welding and a repeated precipitation into a more dispersed form during cooling. Such a transformation of  $\text{CuAl}_2$  particles indicates the formation of a joint through a thin layer of the

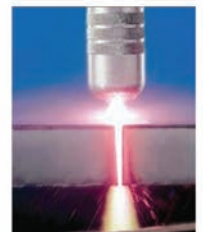
melt, which is a necessary condition for a high-quality welding of aluminium alloys.

4. The ultimate strength of the joints of 15 mm thick plates of 2219-T87 alloy, produced by the developed FBW technology, amounts to 76 % of the base metal of the alloy, both with the arrangement of the weld along and across the rolled metal. The decrease in hardness values in the joint zone is predetermined by the dissolution and coagulation of nanosized strengthening  $\theta'$ -phase.

- Gureeva, M.A., Grushko, O.E. (2009) Aluminium alloys in welded structures of modern transport vehicles. *Mashinostroenie i Inzhenernoe Obrazovanie*, **3**, 27–41 [in Russian].
- Setyukov, O.A. (2013) 1201 aluminium alloy in structure of spacecraft «Buran». *Aviats. Materialy i Tekhnologii*, Special Issue, 15–18 [in Russian].
- Federal aviation administration flight standards service (2018) *Aviation Maintenance Technician Handbook*. [https://www.faa.gov/regulations\\_policies/handbooks\\_manuals/aircraft](https://www.faa.gov/regulations_policies/handbooks_manuals/aircraft).
- ASTM International – Standards Worldwide (2014) *ASTM B209M – 14 Standard Specification for Aluminium and Aluminium-Alloy Sheet and Plate (Metric)*. <https://www.astm.org/Standards/B209M.htm>
- George, E., Totten, G.E. (2003) *Handbook of aluminium*. Vol. 1: Physical metallurgy and processes. Marcel Dekker Inc. New York, NY, USA.
- An, L.H., Cai, Y., Liu, W. et al. (2012) Effect of pre-deformation on microstructure and mechanical properties of 2219 aluminium alloy sheet by thermomechanical treatment. *Transact. Nonferr. Met. Soc. China.*, **22**, 370–375. DOI: [https://doi.org/10.1016/S1003-6326\(12\)61733-6](https://doi.org/10.1016/S1003-6326(12)61733-6).
- Lu, Y., Wang, J., Li, X. et al. (2018) Effects of pre-deformation on the microstructures and corrosion behavior of 2219 aluminium alloys. *Mater. Sci. Eng. A*, **723**, 204–211. doi: 10.1016/j.msea.2018.03.041.
- Sobih, M., Elseddig, Z., Almazy, K., Sallam, M. (2016) Experimental evaluation and characterization of electron beam welding of 2219 Al-alloy. *Indian J. of Materials Sci.*, Article ID 5671532, DOI: <https://doi.org/10.1155/2016/5671532>.
- Huang, C., Kou, S. (2000) Partially melted zone in aluminium welds – liquation mechanism and directional solidification. *Weld J.*, **79(5)**, 113–120.
- Huang, C., Kou, S. (2001) Partially melted zone in aluminium welds: solute segregation and mechanical behavior. *Ibid.*, **80(1)**, 9–17.
- Huang, C., Kou, S. (2001) Partially melted zone in aluminium welds planar and cellular solidification. *Ibid.*, **80(2)**, 46–53.
- Srinivasa, Rao, P., Sivadasan, K.G., Balasubramanian, P.K. (1996) Structure-property correlation on AA 2219 aluminium alloy weldments. *Bull. Mater. Sci.*, **19(3)**, 549–557.
- Poklyatsky, A.G., Chajka, A.A., Klochkov, I.N., Yavorskaya, M.R. (2009) Strength and structure of aluminium alloy welded joints made by friction stir and nonconsumable electrode welding. *The Paton Welding J.*, **9**, 9–12.
- Venkateswarlu, D. (2017) Analysing the friction stir welded joints of AA2219 Al–Cu alloy in different heat-treated state. In: *Proc. of IOP Conf. Series: Mater. Sci. and Eng. (Hyderabad, India, 1–2 June, 2017)*. IOP Publishing. DOI: <https://doi.org/10.1088/1757-899X/330/1/012074>.
- Kang, J., Feng, Z.C., Frankel, G.S. et al. (2016) Friction stir welding of Al alloy 2219-T8: Pt I – Evolution of precipitates and formation of abnormal  $Al_2Cu$  agglomerates. *Metall. Mater. Transact. A*, **47(9)**, 4553–4565. DOI: <https://doi.org/10.1007/s11661-016-3648-7>.
- Kang, J., Feng, Z.C., Li, J.C. et al. (2016) Friction stir welding of Al alloy 2219-T8: Pt II – mechanical and corrosion. *Ibid.*, **47(9)**, 4566–4577. DOI: <https://doi.org/10.1007/s11661-016-3646-9>.
- Kang, J., Liang, S., Wu, A. et al. (2017) Local liquation phenomenon and its effect on mechanical properties of joint in friction stir welded 2219 Al alloy. *Acta Metall. Sin.*, **53(3)**, 358–368. DOI: <https://doi.org/10.11900/0412.1961.2016.00311>.
- Rivera, O.G., Allison, P.G., Brewer, L.N. et al. (2018) Influence of texture and grain refinement on the mechanical behavior of AA2219 fabricated by high shear solid state material deposition. *Mater. Sci. Eng. A*, **724**, 547–558. DOI: <https://doi.org/10.1016/j.msea.2018.03.088>.
- Kuchuk-Yatsenko, S.I. (1992) *Flash butt welding*. Kiev, Naukova Dumka [in Russian].
- Kuchuk-Yatsenko, S.I., Chvertko, P.N., Semyonov, L.A. et al. (2010) Peculiarities of flash butt welding of high-strength aluminium alloy 2219. *The Paton Welding J.*, **3**, 9–12.

Received 05.07.2021

**SEPTEMBER 10, 1957** Plasma cutter was patented. Plasma cutting was invented in 1954 in a laboratory of Linde department of Union Carbide Company. Young scientist Robert Gage found that TIG arc passed through small diameter nozzle significantly rises its intensity and temperature. Passing through this focused arc sufficiently large gas flow, he discovered that such arc can be used for metal cutting. Arc temperature, reaching more than 24000 K, melts metal and intensive air flow blows out molten metal for cutting. Since gas in arc was in overheated state, called plasma, this process was named plasma cutting.



**SEPTEMBER 15, 2014** Huge welding installation was developed at NASA. Vertical assembly platform is a single 170 meter welding aggregate, which was called «Vertical Assembly Center» and located inside the NASA assembly center based in New Orleans. This huge welding installation is designed for welding of lift launch vehicle tank. This development allows successful welding of parts of perspective super heavy — lift launch vehicles that are planned to be used for the most different purposes among which Mars flights.

